Dynamical properties of confined supercooled water: an NMR study



2006 J. Phys.: Condens. Matter 18 S2285

(http://iopscience.iop.org/0953-8984/18/36/S04)

INSTITUTE OF PHYSICS PUBLISHING JOURNAL OF PHYSICS: CONDENSED MATTER

J. Phys.: Condens. Matter **18** (2006) S2285–S2297 doi:10.1088/0953-8984/18/36/S04

# Dynamical properties of confined supercooled water: an NMR study

**Francesco Mallamace[1,2], Matteo Broccio[1,2], Carmelo Corsaro[1], Antonio Faraone[1], Li Liu[1], Chung-Yuan Mou[3] and Sow-Hsin Chen[1]**

[1] Department of Nuclear Science and Engineering, Massachusetts Institute of Technology, Cambridge, MA 02139, USA
[2] Dipartimento di Fisica and CNISM, Università di Messina I-98166, Messina, Italy
[3] Department of Chemistry, National Taiwan University, Taipei, Taiwan

E-mail: francesco.mallamace@unime.it and sowhsin@mit.edu

Received 7 March 2006
Published 24 August 2006
Online at stacks.iop.org/JPhysCM/18/S2285

**Abstract**

We report a set of dynamical data of confined water measured in a very deeply supercooled regime (290–190 K). Water is contained in silica matrices (MCM-41-S) which consist of 1D cylindrical pores with diameters $d = 14, 18$ and 24 Å. When confined in these tubular pores, water does not crystallize, and can be supercooled well below 200 K. We use the NMR technique to obtain the characteristic proton relaxation time-constants (the spin–lattice relaxation time-constant T1 and the spin–spin relaxation time-constant T2) and a direct measurement of the self-diffusion coefficient in the whole temperature range. We give evidence of the existence of a fragile-to-strong dynamic crossover (FSC) at $T_L = 225$ K from the temperature dependence of the self-diffusion coefficient. A combination of the NMR self-diffusion coefficient with the average translational relaxation time, as measured by quasi-elastic neutron scattering, shows a well defined decoupling of transport coefficients, i.e. the breakdown of the Stokes–Einstein relation, on approaching the crossover temperature $T_L$.

(Some figures in this article are in colour only in the electronic version)

## 1. Introduction

It is well known that water is a very mysterious substance, whose properties have intrigued scientists since the last century. Despite its basic importance in science, technology and the environment in daily life, the unusual properties of low-temperature water are far from being completely understood. Therefore, they are currently under active investigation [1–3]. Besides the well known existence of a density maximum at 277 K, many thermodynamic response functions of water, such as isothermal compressibility, isobaric heat capacity, and thermal

  

expansion coefficient, display counterintuitive trends as the temperature is lowered. Bulk water can be supercooled below its melting temperature ($T_M$) down to ≈235 K (its homogeneous nucleation temperature being $T_H = 231$ K), below which it inevitably crystallizes into the hexagonal ice structure (ice-h). In such a metastable supercooled state, the anomalies in thermodynamic properties are most pronounced, showing a power-law divergence toward an apparent singular temperature $T_S \simeq 228$ K. At ambient pressure, water can exist in an amorphous glassy form below $T \approx 135$ K. Depending on $T$ and $P$, glassy water shows a polymorphism, i.e. it has two amorphous phases with different structures: the low- and high-density amorphous ice (LDA and HDA, respectively). In particular, LDA can be formed from HDA and vice versa. LDA, when heated, undergoes a glass-to-liquid transition at $T_G$, transforming into a highly viscous liquid, then crystallizes into cubic ice (ice-c) at $T_X$ (≈150 K). Thus an experimentally inaccessible $T$ region exists in bulk supercooled water between $T_X$ and $T_H$. Experiments performed within this interval could be very useful for understanding the physical origin of the apparent singular temperature $T_S$, giving possible explanations of many open questions concerning the properties of supercooled water. These properties include the location of its $T_G$ (a recent suggestion indicates $T_G \approx 165$ K, if crystallization does not intervene [4]), the existence of a first-order liquid–liquid transition line (LLTL) in the $P$–$T$ plane [5], and the possibility of observing a fragile-to-strong dynamic crossover (FSC) [6]. The existence of the LLTL suggests that the transition between the LDA and HDA is a low-$T$ manifestation of a first-order transition between two distinct liquid water phases: low-density liquid (LDL) and high-density liquid (HDL), of which the LDA and HDA are the corresponding vitreous forms. The transition, marked by the LLTL, terminates at a low-temperature second critical point (predicted to be located at $T_c \approx 220$ K, $P_c \approx 1$ kbar) [3]. At higher temperatures the two liquid phases are indistinguishable. Near this critical point, water is a mixture of both LDA and HDA phases with divergent fluctuation. Lowering temperature or increasing pressure results in the relative increase of the HDA phase with respect to the LDA phase. The FSC can be identified by the temperature at which transport properties, like the shear viscosity $\eta$ and the inverse of the self-diffusion coefficient, cross over from a non-Arrhenius to an Arrhenius behaviour on approaching $T_G$ from above.

A possibility to enter this inaccessible temperature range is now shown by confining water in nanosize pores [7–9]. When contained within these pores, water does not crystallize, and can be supercooled well below $T_H$. Vycor pores [8] (a porous hydrophilic silica glass), micellar systems or layered vermiculite clay [7] are examples of confining nano-structures. The latter system has been used to explore the Arrhenius behaviour of the dielectric relaxation time ($\tau_D$) of water molecules, and thus the strong liquid nature of very deeply supercooled water.

The FSC and its relation to the second critical point was the focus of two very recent studies. The first one uses a high-resolution quasi-elastic neutron scattering (QENS) [10] and the second one uses molecular dynamics (MD) simulations [11]. The MD study shows that for three well known models of water (TIP5P, ST2 and Jagla model), the FSC line coincides with the line of specific heat maxima $C_p^{max}$, called the Widom line. The Widom line is the critical isochore above the critical point in the one-phase region [11]. In particular, it is observed that the crossing of this line is associated with a change in the $T$ dependence of the dynamics. More precisely, the water diffusion coefficient, $D(T)$, changes from non-Arrhenius (*fragile*) to Arrhenius (*strong*) behaviour, while the structural and thermodynamic properties change from those of HDL to those of LDL. In our QENS experiment, the $T$ and $P$ dependences of the average translational relaxation time $\langle \tau_T \rangle$ for water confined in nanopores of silica glass [10] were systematically studied. We showed that as the temperature is lowered, a $\langle \tau_T \rangle$ versus $1/T$ plot exhibits a cusp-like crossover from a non-Arrhenius to an Arrhenius behaviour at a temperature $T_L(P)$. This crossover temperature decreases steadily upon increasing $P$, until it

intersects the $T_H$ line of bulk water at $P \sim 1.6$ kbar. Beyond this point, the FSC can no longer be identified. The neutron scattering experiment was able to locate the end point of the Widom line which is the predicted second critical point of water.

Motivated by these findings, we planned a series of experiments using different techniques, in particular neutron scattering and nuclear magnetic resonance (NMR), to probe dynamical properties of confined water at low temperatures, well inside the inaccessible region for bulk water. The main aim is to clarify water properties, in the light of current theoretical predictions, by measuring the self-diffusion coefficient $D$ directly with NMR, as a function of temperature, and to compare the obtained results with the translational relaxation time $\langle \tau_T \rangle$ measured by QENS.

## 2. Results and discussion

In this paper, we present an NMR study of confined water. The confinement was obtained by using the same silica glass as used in the QENS experiment, i.e. one-dimensional cylindrical nanotubes. We used a micelle-templated mesoporous silica matrix MCM-41-S (having 1D cylindrical tubes arranged in a hexagonal structure), synthesized using the method of zeolite seeds. The pore size was determined using the nitrogen absorption–desorption technique [10]. The investigated samples have hydration levels of $H \simeq 0.5$ (0.5 g $H_2O$ per gram of MCM-41), obtained by exposing dry powder samples to water vapour at room temperature in a closed chamber. As shown by x-ray diffraction (XRD) [12], differential scanning calorimetry (DSC) [13] and NMR [14, 15] experiments, this water-confining system can be regarded as one of the most suitable adsorbent models currently available[4].

Figure 1 shows the first sharp diffraction peak position $Q_0$ (magnitude of the scattering wavevector), measured by an XRD experiment [12], as a function of the temperature of the confined water. It can be seen that water in MCM-41 with a pore diameter of $d = 42$ Å shows a sudden freezing at a temperature of 232 K, whereas for $d = 24$ Å it remains in a liquid state down to ∼160 K. In addition, in the MCM-41-S samples water freezes with a $Q_0$ value which is nearly the same as that of the metastable ice-c ($Q_0^{\mathrm{ice-c}} = 1.7$ Å$^{-1}$) [8, 16], instead of the stable ice-h usually obtained by freezing bulk water ($Q_0^{\mathrm{ice-h}} = 1.6$ Å$^{-1}$) [1]. In both samples, no Bragg peak characteristic of crystallization is observed. The figure also reports the temperature behaviour of $Q_0$ of bulk water (open circles) and of water adsorbed on a mono-layer in Vycor (open triangles) [16]. The DSC curves show, without hysteresis effects, that fully hydrated samples with $d = 29$ and 33 Å exhibit a well defined peak associated with the latent heats of freezing and melting, whereas the $d = 14$ Å sample shows no peak down to 160 K.

The LLTL in water is related to the density of the system. Thus the $Q_0$ data reported in figure 1 give the indication of a structural change of confined water from a higher- to a lower-density form, taking place in the inaccessible region at about $T_S$. In particular, it is evident that the $Q_0$ value measured at the lowest temperatures ($T = 160$ and 232 K for the $d = 24$ and 42 Å samples, respectively) is about the same as that of the LDA phase ($Q_0^{\mathrm{LDA}} = 1.71$ Å$^{-1}$), being $Q_0^{\mathrm{ice-c}} \simeq Q_0^{\mathrm{LDA}}$ [17]. The LDA phase is characterized by the presence of a continuous random hydrogen bond (HB) network in which each water molecule is locally engaged in four hydrogen

[4] The geometrical constraints and chemistry of the hosting material surface may significantly affect the structure and dynamics of confined water. Some examples are pore channel intersections (with networking effects), pore polydispersity, charges and chemical impurities. These phenomena are revealed by a marked hysteresis in the cooling/warming cycle of confined water: they are absent, or negligible, in MCM-41 nanotube samples studied here, as shown by XRD [12] and DSC experiments [13]. DSC also shows that repeated freezing and melting cycles (FMCs) did not cause any significant change in the position and shape of DSC peaks for a given sample. The melting temperature was reproducible even after several months. Therefore, in repeated FMCs, water does not affect the pore walls in these silica samples.

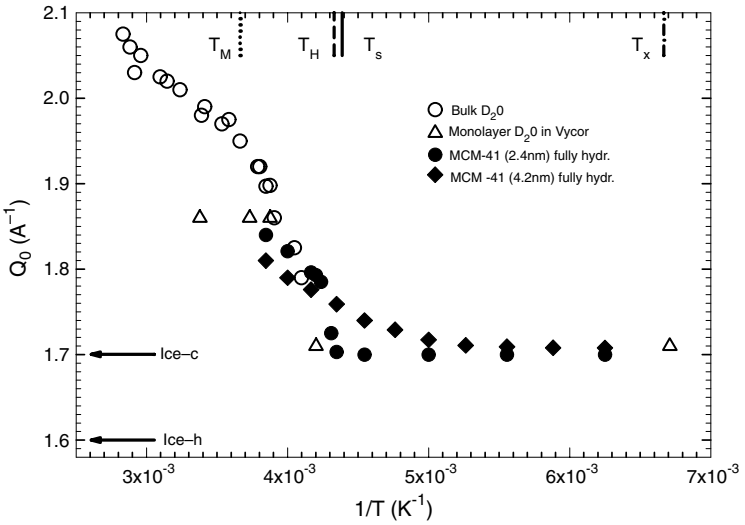


**Figure 1.** Scattered wavevector position ($Q_0$) of the first diffraction peak, versus $1/T$, of bulk water (open circles), $D_2O$ monolayer in Vycor (open triangles), water in fully hydrated MCM-41-S samples with a pore diameter of $d = 41$ Å (dark circles) and $d = 24$ Å (dark diamonds). For comparison the $Q_0$ values measured in ice-c and ice-h are reported.

bonds [17]. Thus the overall behaviour of the $Q_0$ data (reported in figure 1(b)) suggests that the $d = 24$ Å sample can be used to explore the properties of liquid water from above $T_M$ to well inside the inaccessible temperature region.

The dynamical properties of water confined in fully hydrated MCM-41-S samples with $d = 24, 18$ and 14 Å have been studied at ambient pressure and different temperatures by using a Bruker AVANCE NMR spectrometer operating at 700 MHz $^1$H resonance frequency. In these NMR experiments, we have measured the self-diffusion coefficient of water $D$, the proton relaxation time-constants (the spin–lattice $T_1$ and the spin–spin $T_2$), the apparent spin–spin relaxation time $T_2^*$, and the maximum intensity $I^{max}$ of the $^1$H-NMR spectra (obtained from the free-induction decay (FID)). The explored temperature range was 190–298 K (with an accuracy of ±0.2 K). The $T$-dependence of the chemical shift of methanol was used as a $T$-standard. Samples have been studied by cooling or heating cycles which result in the same spectra. Usually, we started from 296 K and cooled the samples in steps of 5 K down to 180 K; after that the procedure was reversed. Before starting with the heating process, samples were kept for some hours at $T = 180$ K. $D$ was measured with the pulsed gradient spin-echo technique ($^1$H-PGSE) [18]. For the measurement of $T_1$ and $T_2$, we used the standard inversion recovery pulse sequence ([$\pi$–$t$–$\pi/2$–acquisition], $t$ denoting the time between the two RF pulses) and the Carr–Purcell–Meinboom–Gill (CPMG) pulse sequence [18], respectively.

In general, the $^1$H relaxation in confined water systems is characterized by three contributions, coming from the inner confined bulk water (ICBW), the water molecules close to the adsorbent surface (SW), and the protons of silanol groups on the silica surface. A characteristic of MCM materials is that only ICBW (having a $T_1$ value comparable to that of bulk water) [14, 15] and SW protons contribute to the NMR spectra, and these contributions can be studied separately [19]. We will consider only the ICBW dynamics in the following. PGSE self-diffusion measurements are based on NMR pulse sequences which generate a spin-echo of the magnetization of the resonant nuclei. By appropriate addition of pulsed field gradients (PFG) of duration $\delta$, intensity $g$ and interval $\Delta$ in the defocusing and focusing period of the

sequence, the spin-echo becomes sensitive to the translational motion of molecules carrying the nuclear spin under investigation. In stochastic processes, such as thermally excited Brownian motion (self-diffusion), the spin-echo intensity $M(\delta g, \Delta)$ is attenuated. The attenuation factor is usually given in terms of the mean square displacement $\langle r^2(\Delta)\rangle$ of the diffusing molecules, along the PFG direction **r**, during the time interval $\Delta$ by

$$\Psi(\delta g, \Delta) = M(\delta g, \Delta)/M(0, \Delta) = \exp[-(\gamma \delta g)^2 (1/2) \langle r^2(\Delta)\rangle]. \quad (1)$$

$\gamma$ is the gyromagnetic ratio of the observed nucleus ($\gamma(^1\mathrm{H}) = 2.67 \times 10^8$ (T s)$^{-1}$) and $q = \gamma \delta g$ the magnitude of the wavevector. In general, one may define a time-dependent self-diffusion coefficient $D(\Delta)$ through the relation $\langle r^2(\Delta)\rangle = 2D(\Delta)\Delta$, from which the long-time limit $D$ is obtained. Considering the system properties, we have used a proper procedure for the measurements of the self-diffusion coefficient, discussed in the next.

The $^1$H NMR spectra (obtained from the FID) of water in MCM samples with $d = 24$ and 14 Å upon cooling are shown in figures 2(a) and (b), respectively. The full width at half height of these spectra, $\Delta\nu_{1/2} \sim 1/T_2^*$, is the rate of the so-called *apparent* spin–spin relaxation, having time-constant $T_2^*$, which is related to the spin–spin relaxation time-constant $T_2$. As can be observed, the maximum intensity of the spectra ($I^{\max}$) decreases and the corresponding linewidth increases upon decreasing $T$. The crystalline ice phase (characterized by a very large linewidth) is not observed. From these data, by using a proper fitting procedure, we obtained both $T_2^*$ and $I^{\max}$. We stress that the same spectra are obtained after heating the samples up starting from 180 K and keeping them at this temperature for some hours; thus hysteresis effects in the cooling/warming cycle of confined water are absent (see footnote 1). The obtained $T_2^*$ and the corresponding $T_2$ values for water in MCM-41-S nanotubes with $d = 24$ and 12 Å are plotted against $1/T$ in figure 3(a). In all the studied temperature range these quantities are characterized, in the cooling process, by a gradual decrease from 500 to about 150 $\mu$s. It has to be noticed that the value corresponding to bulk ice is about 10 $\mu$s. In addition, as can be observed, these quantities are independent, within the experimental error, of the tube sizes, indicating the same 'transverse' spin–spin dynamics.

The NMR signal intensity is directly related to the system equilibrium magnetization, $M_0$ (or the susceptivity $\chi_0$), which depends linearly on the total number of mobile spins per unit volume, on the mean square value of nuclear magnetic moment and on $1/T$ (Curie law). Figure 3(b) shows $I^{\max}$, for $d = 14, 18$ and 24 Å samples, upon both cooling and heating, corrected for the Curie effect and normalized to the pore volume, as $I_{\mathrm{Nor}}^{\max}$ versus $1/T$. As can be noticed, the $T$ behaviour of confined water is independent of the pore size.

The figure clearly shows a steep decrease of $I_{\mathrm{Nor}}^{\max}$ on decreasing $T$, at ∼225 K ($T_{\mathrm{L}}$). This indicates that $T \sim 225$ K is a crossover temperature for the dynamical behaviour of water. In general, relaxations measured in an NMR experiment are caused by random fluctuations of the magnetic field at the position of a resonating spin originating from the thermal motion of neighbouring spins. In our case ($T_2^*$ relaxation) the fluctuating magnetic dipole–dipole interactions between $^1$H spins are due to the tumbling of molecules under the local caging structure. Hence the observed behaviour of $I_{\mathrm{Nor}}^{\max}$ can be related to the structure of water and in particular to its packing density. The existence of an LLTL and the associated second critical point in water is based on the idea that water can exist in two liquid structures: a low-density liquid (LDL, where the locally tetrahedrally coordinated hydrogen bond (HB) network is fully developed) and a high-density liquid (HDL, where the HB network is not fully developed) [1, 3]. The probability of tumbling of a water molecule is higher in the HDL phase compared to that in the LDL phase, and the temperature behaviour of $I_{\mathrm{Nor}}^{\max}$ shown in figure 3(b) reflects just this situation, indicating $T \sim 225$ K as the crossover temperature between the HDL and the LDL.

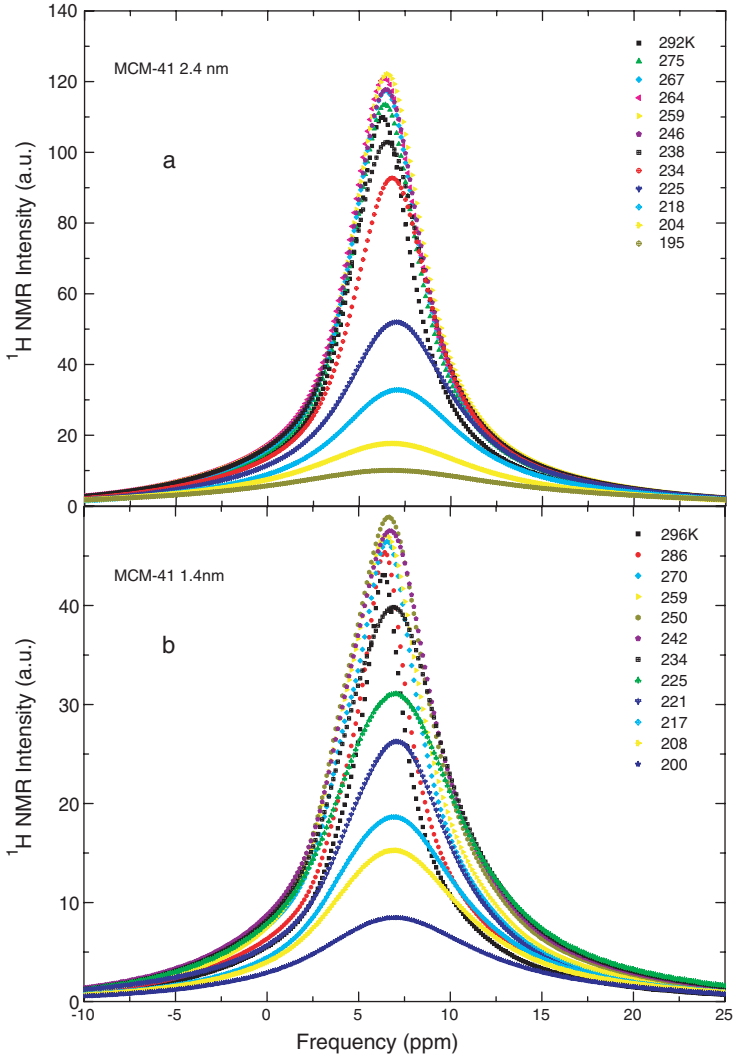


**Figure 2.** The $^1$H NMR spectra, obtained by the FID, of water in MCM-41-S nanopores with $d = 24$ Å (a) and 14 Å (b) at different temperatures.

Figure 4 reports the $T_1$ curves for water in samples with $d = 24$ Å (figure 2(a)) and 14 Å (figure 2(b)). All these spectra are well fitted by a single-exponential form in the whole range 215–296 K, whereas for $T < 215$ K an additional contribution emerges, whose weight is at most a few per cent of the total (this may be due to the presence of a very small amount of metastable ice). $T_1$ at room temperature is $\simeq$1 s, i.e. of the same order of magnitude as bulk water (3 s), whereas on decreasing $T$ it decreases to $\simeq$0.5 s (at 215 K). These results, namely a single-exponential decay from $T = 296$ K down to the deeply supercooled temperature 215 K along with the values of $T_1$, suggest that the ICBW under study bears strong similarities with bulk water.

Recently, the NMR technique was used to study structural and dynamical properties of liquid confined in porous material. The spin-echo method, measuring the signal amplitude

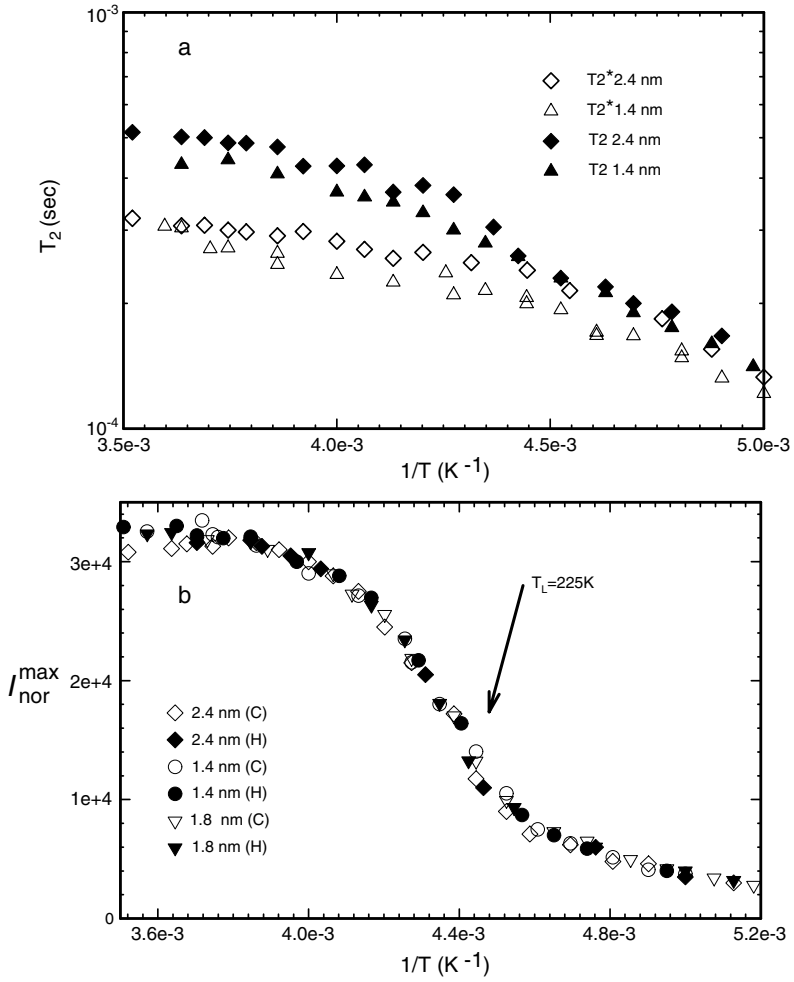


**Figure 3.** (a) The spin–spin ($T_2$) and the apparent spin–spin ($T_2^*$) relaxation times of water in MCM-41-S nanotubes with $d = 24$ and 12 Å versus $1/T$. (b) The peak intensities of the $^1$H NMR spectra (water in nanotubes with $d = 24$, 18 and 14 Å), corrected for the Curie law and normalized to the pore volume, $I_{\mathrm{Nor}}^{\mathrm{max}}$ versus $1/T$. Open and closed symbols indicate the intensities measured in the cooling and heating phases, respectively. The arrow indicates the location of the crossover temperature $T_{\mathrm{L}} \simeq 0.225$ K.

in a $[\pi/2\text{–}t\text{–}\pi]$ sequence, was used to characterize the pore size distribution of porous silica materials in the range 5 nm $< d <$ 50 nm [20]. Another experiment reports pulsed field gradient NMR self-diffusion of water adsorbed in MCM-41 materials with $d \approx 1$ $\mu$m [21]. This latter experiment suggests that the measured $D$ may be influenced by the geometry of the host matrix. In particular, the diffusion process may be dominated by 'anisotropic effects' caused either by the permeability to water of the pore walls or by the distortion and bending of channels over the probed diffusion length. These results are controversial, compared with the findings of a study considering the anomalous diffusion of small molecules in random networks and the associated signal attenuation seen in NMR field gradient spectroscopy. In particular, in the case of field gradient pulses with short duration ($\delta \ll \Delta$), the decay form of spin-echo amplitude $\Psi(\delta g, \Delta)$ is formally identical to the expression for ordinary diffusion [22].

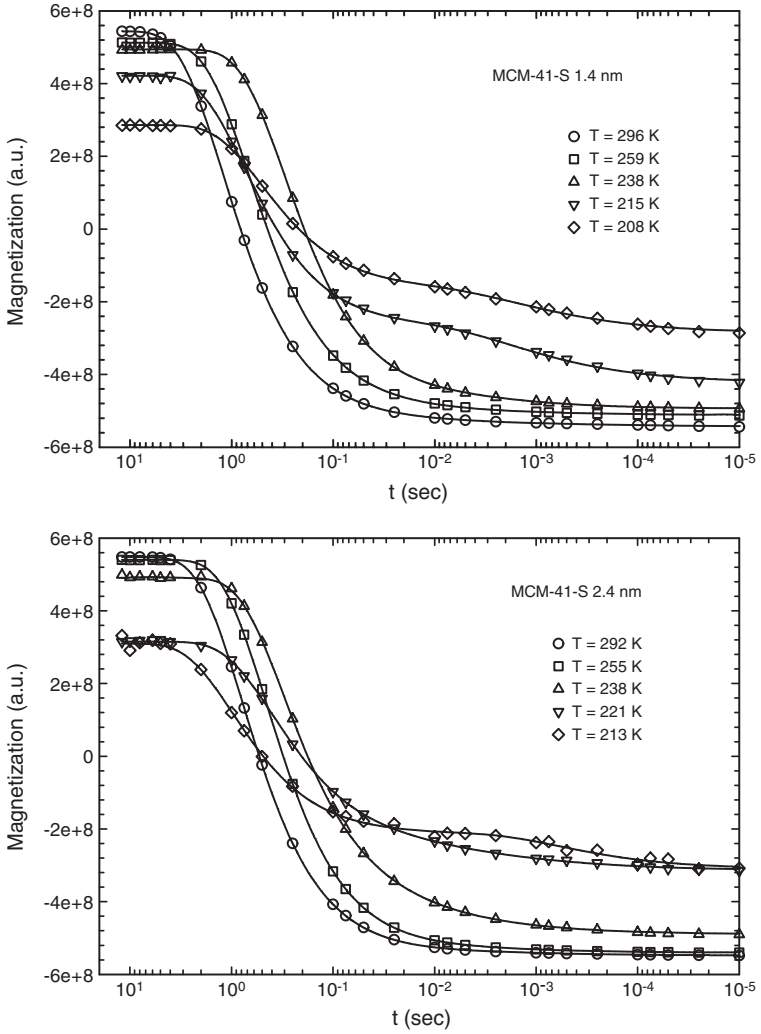


**Figure 4.** Amplitudes, at different temperatures, of the raw spin–lattice magnetization recoveries, versus time, for water confined in MCM-41-S samples with $d = 14$ Å (upper panel) and 24 Å (lower panel). Solid lines, in the range 296–215 K are the fits with a single exponential function.

This event is also taken into account by spectroscopic and scattering methods, considering the dependence of the measured mean line-width ($\Gamma = Dq^2$) on the probing wavevector ($q = \gamma\delta g$ for NMR experiments) for a system with characteristic length scale $\lambda$. More precisely, there are mainly two situations, depending on the $q\lambda$ value: for $q\lambda \ll 1$ (the probe window $q^{-1}$ being larger than the characteristic length scale) the measured $D$ is independent of $q$; in the opposite case $q\lambda \gg 1$ (probe size shorter than $\lambda$) $D$ is influenced by the system structure.

Our previously reported data of $T_1$, $T_2$ and $I_{\mathrm{Nor}}^{\mathrm{max}}$ give a general picture that agrees with this latter consideration: field gradient NMR experiments whose probed length scale is longer than pore sizes give $D$ values unaffected by the geometry of the matrix, in particular considering that the dynamical quantities $T_1$ and $T_2$ are strongly related to the system viscosity [23]. However, special care must be taken in dynamical measurements involving

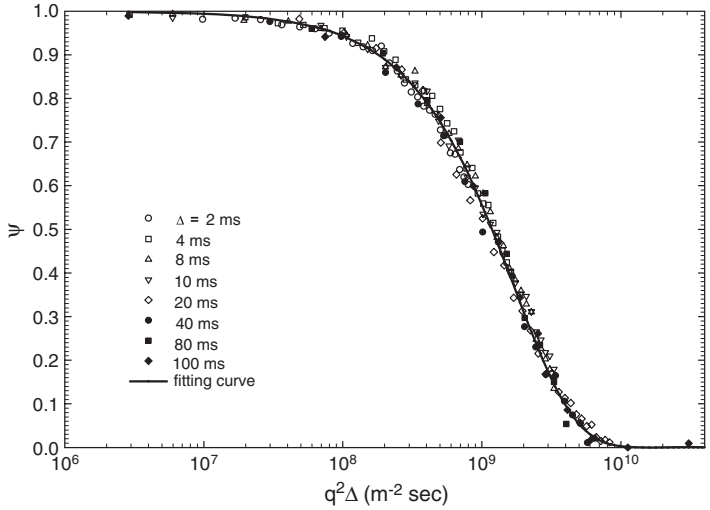


**Figure 5.** The typical normalized spectrum of the attenuation of $\Psi(\delta g, \Delta)$ of water confined in an MCM-41-S sample with $d = 14$ Å for $T = 270$ K. The spectrum was obtained by collecting seven measurements with the same $\delta = 2$ ms and the following $\Delta$ values: $\Delta = 4, 8, 10, 20, 40, 80, 100$ ms. The continuous line represents the data fitting with a stretched exponential form.

'complex materials', particularly in supercooled liquids or glass forming materials that, as is well known, are characterized by multi-relaxations and non-ergodic properties. For these systems, the attenuation of the spin-echo amplitude, $\Psi(\delta g, \Delta) = M(\delta g, \Delta)/M(0, \Delta)$ is expected to decay not in accordance with equation (1) (single exponential) but with stretched exponential or power law forms. In order to have a good statistics for a correct evaluation of the corresponding self-diffusion coefficient $D(\Delta)$, we performed more than 100 measurements for each temperature, at various values of $\delta$ and $\Delta$. In particular, each $\Psi$ spectrum was obtained for different $\Delta$ values at a fixed $\delta$. Figure 5 reports in a linear–log plot versus $q^2\Delta$ a typical normalized spectrum of the attenuation of $\Psi(\delta g, \Delta)$ of water confined in an MCM-41-S sample with $d = 18$ Å, for $T = 270$ K; the spectrum was obtained by collecting eight measurements with the same $\delta = 0.2$ ms and the following $\Delta$ values: $\Delta = 2, 4, 8, 10, 20, 40, 80, 100$ ms.

The data reported in figure 5, like all the obtained spectra, have been fitted using the stretched exponential form: $\Psi(\delta g, \Delta) = \exp[-(q^2\widetilde{\Delta}D_e)^\beta]$, where $\widetilde{\Delta} = (\Delta - \delta/3)$, $\beta$ $(0 < \beta < 1)$ measures the width of the self-diffusion coefficient distribution, while $D_e$ is some effective self-diffusion coefficient. A mean self-diffusion coefficient can be calculated from the relation $1/D = (1/\beta)\Gamma(1/\beta)(1/D_e)$. Fitting the data reported in figure 5, we obtained $\beta = 0.7$ and $D \simeq 7.5 \times 10^{-10}$ (m$^2$ s$^{-1}$). For each temperature, the $D$ values of the corresponding $\Psi$ spectra obtained with such a procedure have been averaged and then plotted versus $1/T$ in figure 6.

Figure 6 shows, in a log–linear plot versus $1/T$, the self-diffusion coefficient $D$ measured in the present NMR experiment on water in MCM nanopores of 14 Å (open squares) and, for comparison, that of supercooled pure bulk water (open circles), measured with the same technique [24]. We stress that each data point in this figure is the average over a large set of data obtained at the same $T$ from many distinct $\Psi$ spectra having different $\delta$ and $\Delta$, under the condition $\delta \ll \Delta$. The $T$ behaviour of the pure bulk water was fitted with a Vogel–Fulcher–Tamman (VFT) law $D = D_0 \exp\left[-BT_0/(T - T_0)\right]$ (as shown by the solid line), where $B$

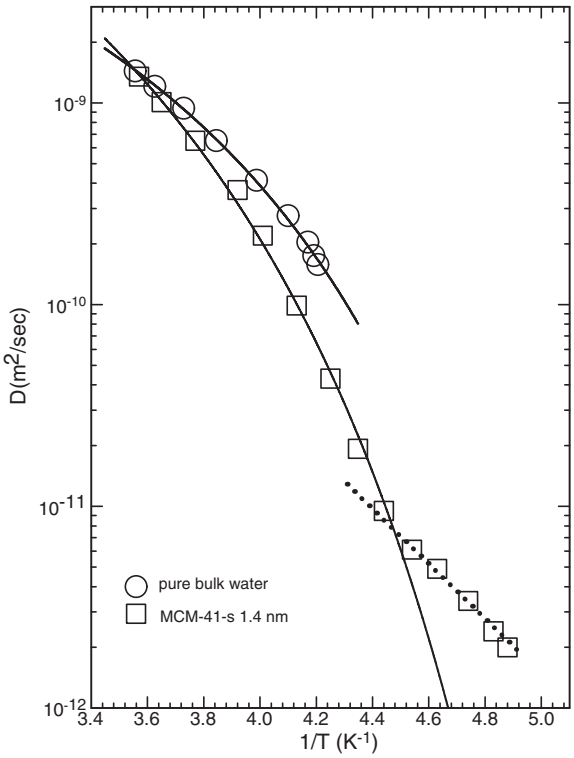


**Figure 6.** The NMR water self-diffusion coefficient $D$ ($m^2\ s^{-1}$) as a function of $1/T$. Open squares represent the diffusion coefficient of water confined in MCM nanotubes with a pore diameter of 14 Å, whereas open circles are the NMR data measured in pure bulk water above $T_H$. Continuous and dotted lines are a guide for the eyes.

is a constant providing a measure of the system fragility and $T_0$ the ideal glass transition temperature; obtained values are $D_0 = 4 \times 10^{-8}\ m^2\ s^{-1}$ $B = 2, 3$ and $T_0 = 169.7$ K. The solid and dotted lines drawn on top of the confined water data clearly indicate that $T \sim 225$ K is a crossover temperature, below which the diffusion constant behaves according to an Arrhenius law whereas above is non-Arrhenius. So these $D$ data confirm directly, according to QENS data [10] and MD simulation results [11], that dynamical properties of this type of confined water are characterized by the presence of an FSC.

To clarify, in a quantitative way, the physical properties of confined water underlying the reported NMR data, a good approach is represented by a comparative analysis with the QENS data from the same sample, in analogous conditions of temperature and pressure. Figure 7 shows, for the fully hydrated MCM-41-S samples with $d = 14$ Å, a plot as a function of $T_0/T$ of the inverse of the self-diffusion coefficient of water $(1/D)$ measured by NMR in a log–linear scale (panel (a)), and the average translational relaxation time $\langle \tau_T \rangle$ obtained by analyses of QENS spectra using relaxing cage model (RCM) (panel (b)). In panel (a), the long dashed line denotes the fit of the data to a Vogel–Fulcher–Tamman (VFT) law $1/D = 1/D_0 \exp(BT_0/(T - T_0))$, where $1/D_0 = 3.58 \times 10^6\ s\ cm^{-2}$, $B = 3.07$, and $T_0 = 172$ K. The short dotted line denotes the fit to an Arrhenius law $1/D = 1/D_0 \exp(E_A/k_B T)$, where we keep the same $1/D_0$ value as in the VFT law fit, and $E_A = 4.69$ kcal $mol^{-1}$. Panel (b) shows the $\langle \tau_T \rangle$ data at ambient pressure. The dashed lines denote the VFT law fit, and the

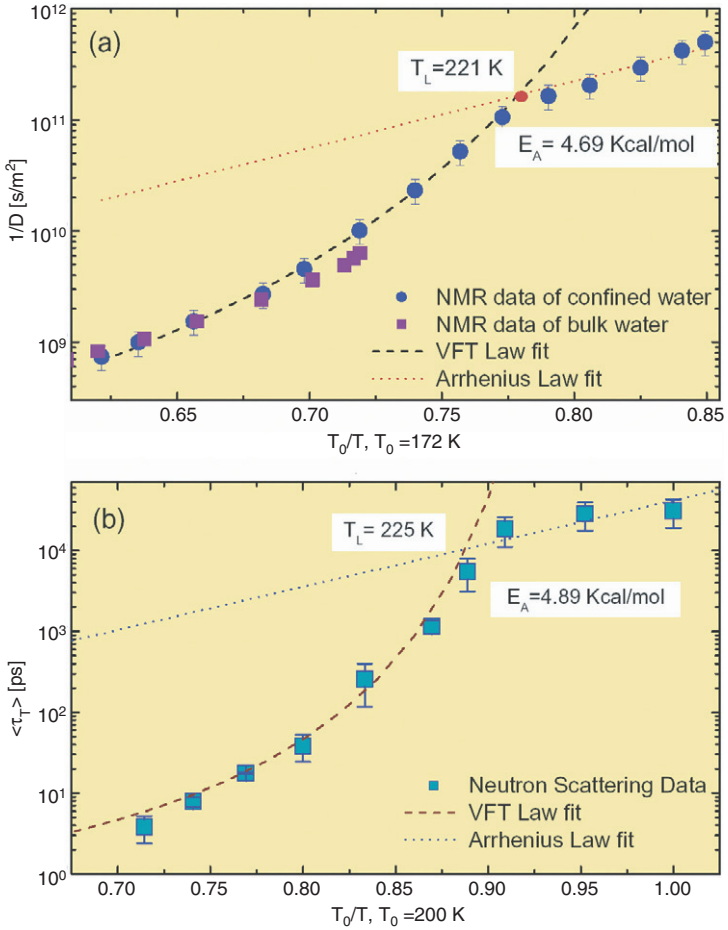


**Figure 7.** Panel (a) reports the inverse of the NMR self-diffusion coefficient $\log(1/D)$, versus $T_0/T$, plot for water in MCM-41-S with 14 Å pores. In the same panel are indicated the same quantities measured in bulk water (full squares). In panel (b) are plotted the average translational relaxation time $\langle \tau_T \rangle$ measured by neutron scattering (QENS) as a function of $T_0/T$. In both cases dashed lines denote the Vogel–Fulcher–Tamman (VFT) law fit and the dotted lines denote the Arrhenius fit with the same prefactor.

dotted lines the Arrhenius law fit, with the same prefactor $\tau_0$. We obtained the following values: $E_A = 4.89$ kcal mol$^{-1}$, $T_0 = 200$ K. The consequence of insisting on the same prefactor in both the VFT and the Arrhenius laws results in an equation determining the crossover temperature $T_L$ in the following form: $1/T_L = 1/T_0 - Bk_B/E_A$. We thus obtained $T_L = 223 \pm 2$ K from the $1/D$ data and $T_L = 225$ K from the $\langle \tau_T \rangle$ data.

The agreement between NMR and QENS results is thus satisfactory, especially regarding the two relevant quantities $E_A$ and $T_L$. As previously mentioned, for water, which is fragile at room and at moderately supercooled temperatures, an FSC occurring at 228 K has been proposed on the basis of thermodynamic arguments by Ito *et al* [6]. The interpretation of this transition as a variant of the structural arrest transition (as predicted by the ideal mode coupling theory) was the essence of the recent QENS study of the structural relaxation time and MD study of the self-diffusion coefficient [10, 11]. The NMR results presented above constitute,

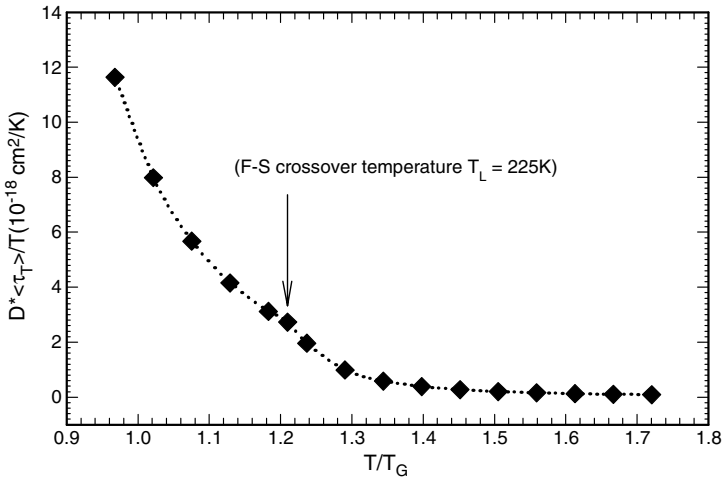


**Figure 8.** $D\langle\tau_T\rangle/T$ versus $T/T_{\rm G}$. The deviation from constancy of such a quantity indicates the violation of the Stokes–Einstein relation in supercooled water. We assume, from literature data, $T_{\rm G} = 186$ K.

therefore, an independent confirmation of the existence of FSC at ambient pressure, by means of a direct measurement of the self-diffusion coefficient of supercooled water.

The NMR and QENS data obtained separately can be used to verify the existence for water of important properties characterizing glass forming materials. The dynamical properties of this system on approaching the glass transition are essentially different from normal liquids, which exhibit homogeneous behaviour over length scales larger than the correlation length of density fluctuations. Despite many efforts, a complete understanding of the dynamical properties on a molecular scale underlying the glass transition is not yet established. There are some experimental observations of dynamics in deeply supercooled liquids which are unexpected if compared with normal or high-temperature fluids. An intriguing example is represented by the well known Stokes–Einstein (SE) equation, which relates the self-diffusion constant $D$, viscosity $\eta$ and temperature $T$ ($D \sim T/\eta$). For normal liquids the SE relation is usually accurate and gives a reasonable description of these systems, whereas for some supercooled liquids it has been observed that the product $D\eta$ increased by some order of magnitude as the temperature was lowered, approaching $T_{\rm G}$ [25, 26]. These results indicate a decoupling of translational diffusion from viscosity or rotational diffusion. The NMR and QENS data of confined water presented above allows us to verify whether water in the supercooled regime shows the breakdown of the SE relation on approaching $T_{\rm G}$ [28]. Since the translational relaxation time $\langle\tau_T\rangle$, or equivalently the structural relaxation time, is proportional to the viscosity $\eta$, if the SE relation is obeyed, then $D\langle\tau_T\rangle/T \sim$ const. This quantity (calculated by the $D$ obtained from NMR and the corresponding $\langle\tau_T\rangle$ obtained from QENS for the $d = 14$ Å MCM-41-S) is shown in figure 8 as a function of temperature $T_{\rm G}$. The figure shows that this quantity is indeed constant at higher $T$, but it increases steeply as $T$ goes below the FSC temperature. It further shows, as predicted by the theory, a small blip just at the FSC temperature. In reference [27], focusing on the study of the decoupling of transport coefficients in supercooled liquids, the breakdown of the SE relation in structural glass formers is attributed to the enhancement of 'dynamical heterogeneities' in the supercooled liquid.

## 3. Conclusion

In conclusion, our NMR results show that confined water in the supercooled regime is characterized by the existence of a fragile-to-strong crossover. Their combination with QENS data highlights the physical picture that the water structure evolves, upon decreasing $T$, from an HDL phase, characterized by a fragile behaviour, to an LDL phase, characterized by a strong behaviour, before it reaches the glass transition temperature $T_G$. In addition, we also showed that the water dynamics is characterized by the breakdown of the Stokes–Einstein (SE) relation, i.e. a manifestation of the decoupling of translational diffusion coefficient from shear viscosity or rotational diffusion coefficient.

## Acknowledgments

The research at MIT is supported by a grant from the Materials Science Division of US DOE. The research in Messina is supported by the MURST-PRIN2004. We benefited from affiliation with the EU Marie Curie Research and Training Network on Arrested Matter. We acknowledge a fruitful discussion with Dr J P Garrahan on the breakdown of the Stokes–Einstein relation.

## References

[1] Angell C A 1982 *Water: a Comprehensive Treatise* vol 7, ed F Franks (New York: Plenum) pp 1–81
[2] Mishima O and Stanley H E 1998 *Nature* **396** 329
[3] Debenedetti P G and Stanley H E 2003 *Phys. Today* **56** 40
[4] Velikov V, Borick S and Angell C A 2001 *Science* **294** 2335
[5] Poole P H, Sciortino F, Essmann U and Stanley H E 1992 *Nature* **360** 324
[6] Ito K, Moynihan C T and Angell C A 1999 *Nature* **398** 492
[7] Bergman R and Swenson J 2000 *Nature* **403** 283
[8] Dore J 2000 *Chem. Phys.* **258** 327
Webber B and Dore J 2004 *J. Phys.: Condens. Matter* **16** S5449
[9] Koga K, Tanaka H and Zeng X C 2000 *Nature* **408** 564
[10] Faraone A *et al* 2004 *J. Chem. Phys.* **121** 10843
Liu L *et al* 2005 *Phys. Rev. Lett.* **95** 117802
[11] Xu L, Kumar P, Buldirev S V, Chen S-H, Poole P H, Sciortino F and Stanley H E 2005 *Proc. Natl Acad. Sci. USA* **102** 16558
[12] Morishige K and Nobuoca K 1997 *J. Chem. Phys.* **107** 6965
[13] Schreiber A, Ketelsen I and Findenegg G H 2001 *Phys. Chem. Chem. Phys.* **3** 1185
[14] Overloop K and Van Gerven L 1993 *J. Mag. Res.* A **101** 147
[15] Hansen E W, Schmidt R, Stöcker M and Akporiaye D 1995 *J. Phys. Chem.* **99** 4148
[16] Zanotti J M, Bellissent-Funel M C and Chen S H 2005 *Europhys. Lett.* **71** 91
[17] Bellissent-Funel M-C, Teixeira J and Bosio L 1987 *J. Chem. Phys.* **87** 2231
Bellissent-Funel M-C, Bosio L, Hallbrucker A, Mayer E and Sridi-Dorbez R 1992 *J. Chem. Phys.* **97** 1282
[18] Stejskal E O and Tanner J E 1964 *J. Chem. Phys.* **42** 288
Price W S 1998 *Concepts Mag. Reson.* **10** 197
[19] Grünberg B, Emmler T, Gedat E, Shenderovich J, Findenegg G H, Limbach H H and Buntkowsky G 2004 *Chem. Eur. J.* **10** 5689
[20] Strange J H, Rahman M and Smith E G 1993 *Phys. Rev. Lett.* **21** 3589
Mitzthras A and Strange J H 1994 *Magn. Res. Imag.* **12** 261
[21] Stallmach F, Kaerger J, Krause C, Jeschke M and Oberhagemann U 2000 *J. Am. Chem. Soc.* **122** 9237
[22] Kärger J, Pfeifer H and Vojta G 1988 *Phys. Rev.* A **11** 4514
[23] Bloembergen N, Purcell E M and Pound R V 1948 *Phys. Phys. Rev.* **73** 679
[24] Price W S, Hiroyudi I and Arata Y 1999 *J. Phys. Chem.* A **103** 448
[25] Swallen S F, Bonvallet P A, McMahon R J and Ediger M D 2003 *Phys. Rev. Lett.* **90** 015901
[26] Fujara F, Geil B, Sillescu H and Fleishcer G 1992 *Z. Phys.* B **88** 195
[27] Ediger M D 2000 *Ann. Rev. Phys. Chem.* **51** 99
[28] Jung Y-J, Garrahan J P and Chandler D 2004 *Phys. Rev.* E **69** 061205